



OPEN

Transcriptome, hormonal, and secondary metabolite changes in leaves of *DEFENSE NO DEATH 1 (DND1)* silenced potato plants

Zsófia Bánfalvi^{1,3}✉, Balázs Kalapos², Kamirán Áron Hamow^{2,3}, Jeny Jose^{1,2,3}, Csaba Éva^{2,3}, Khongorzul Odgerei^{1,3}, Flóra Karsai-Rektenwald^{1,3}, Vanda Villányi^{1,3} & László Sági^{2,3}

DEFENSE NO DEATH 1 (DND1) is a cyclic nucleotide-gated ion channel protein. Earlier, it was shown that the silencing of *DND1* in the potato (*Solanum tuberosum* L.) leads to resistance to late blight, powdery mildew, and gray mold diseases. At the same time, however, it can reduce plant growth and cause leaf necrosis. To obtain knowledge of the molecular events behind the pleiotropic effect of *DND1* downregulation in the potato, metabolite and transcriptome analyses were performed on three *DND1* silenced lines of the cultivar 'Désirée.' A massive increase in the salicylic acid content of leaves was detected. Concentrations of jasmonic acid and chlorogenic acid and their derivatives were also elevated. Expression of 1866 genes was altered in the same way in all three *DND1* silenced lines, including those related to the synthesis of secondary metabolites. The activation of several alleles of leaf rust, late blight, and other disease resistance genes, as well as the induction of pathogenesis-related genes, was detected. *WRKY* and *NAC* transcription factor families were upregulated, whereas *bHLHs* were downregulated, indicating their central role in transcriptome changes. These results suggest that the maintenance of the constitutive defense state leads to the reduced growth of *DND1* silenced potato plants.

Keywords *Solanum tuberosum*, Salicylic acid, Differentially expressed genes, Disease resistance genes, Metabolite analysis

Crops are exposed to many diseases, which cause substantial economic losses worldwide. Breeding for disease-resistant varieties offers the most economic and environmentally friendly means of disease control. To date, breeders have focused mainly on the introgression of resistance genes in elite genotypes. These genes, however, often confer race-specific resistance and are not durable because they are frequently overcome by a new, virulent race of a pathogen; in contrast, the silencing or mutating of susceptibility genes, which pathogens require to establish a compatible interaction with the host, are expected to lead to durable resistance¹.

The *DEFENSE NO DEATH 1 (DND1)* gene encodes a cyclic nucleotide-gated ion channel protein². It was discovered in *Arabidopsis thaliana* that mutants in the *DND1* locus are defective in hypersensitive response but exhibit enhanced resistance against a broad spectrum of virulent fungal, bacterial, and viral pathogens in correlation with the elevated levels of salicylic acid (SA) compounds and mRNAs for pathogenesis-related (PR) genes. As a pleiotropic effect of the above changes these mutants also exhibit a dwarfed rosette phenotype³. Interestingly, mutations that affect SA accumulation or signalling abolish the enhanced resistance of *dnd1* mutants against *Pseudomonas syringae* and *Hyaloperonospora parasitica* but not *Botrytis cinerea*; this suggests that the broad-spectrum resistance of *dnd1* mutants is related to the activation or sensitization of multiple defense pathways⁴. *DND1* conducts Ca^{2+} into cells and links the Ca^{2+} flow to the downstream production of nitrogen oxide (NO), which is an essential signalling molecule invoking plant innate immune response to pathogens⁵. NO is a central component of the plant senescence signalling cascades. Investigation of *dnd1* mutants revealed an interrelationship between Ca^{2+} and NO generation in leaf cells during senescence. Endogenous NO content in *dnd1* leaves is lower than in leaves of wild-type, and these plants show a series of early senescence phenotypes^{6,7}.

¹Department of Plant Biotechnology, Institute of Genetics and Biotechnology, Hungarian University of Agriculture and Life Sciences, Gödöllő, Hungary. ²Agricultural Institute, HUN-REN Centre for Agricultural Research, Martonvásár, Hungary. ³Agribiotechnology and Precision Breeding for Food Security National Laboratory, Martonvásár, Hungary. ✉email: banfalvi.zsophia@uni-mate.hu

Besides early senescence, *dnd1* mutant *Arabidopsis* plants flower significantly later, indicating the dependence of flowering time on Ca^{2+} signalling⁸. This phenotype, however, is independent of SA or SA signalling⁹.

The essential role of *DND1* in resistance to phytopathogens has been established in non-model and crop plants, too. Homologs of the *Arabidopsis* *DND1* are expressed early during infection by the rust fungus *Hemileia vastatrix* in coffee¹⁰. In the potato and tomato, down-regulation of *DND1* leads to resistance to late blight (*Phytophthora infestans*) and to powdery mildew species, *Oidium neolycopersici* and *Golovinomyces orontii*, and impedes the conidial germination, attachment, and hyphal growth of *Botrytis cinerea*^{11,12}. The tetra-allelic *DND1* gene-edited potato lines confer increased late blight resistance. These lines, however, like the *DND1* silenced lines¹¹, show reduced growth and leaf necrosis¹³. Thus, it was concluded that due to the pleiotropic phenotypes observed, *DND1* is not a good candidate for application in agriculture¹³. Nevertheless, *DND1* may activate multiple defense pathways in the potato, one or more of which may be separable from the one with the pleiotropic effect, as was demonstrated in *A. thaliana*⁴.

To get a general overview on the molecular basis of the pleiotropic effect of *DND1* silencing this study aimed to obtain knowledge at three levels and detect transcriptomic, hormonal, and secondary metabolite changes in potato leaves. Here, we report the elevation of SA concentration, the upregulation of 1138 genes, and the downregulation of 728 genes in three *DND1* silenced potato lines generated earlier¹¹. The effects of transcriptional and metabolite changes on the growth and fungal resistance of *DND1* silenced lines are discussed.

Results

Re-testing and targeted hormone and metabolite analysis of the *DND1* silenced potato lines

The *DND1* silenced lines DND1-5, DND1-8, and DND1-17 were transferred from Wageningen University, The Netherlands, to our laboratory. To test whether, after propagation in vitro, the transferred lines retained their reduced level of *DND1* expression¹¹, RNA was isolated from the leaves of in vitro plants, and the level of *DND1* mRNA in comparison to that of the non-transformed control 'Désirée' (DES) was tested with RT-qPCR. A 50–60% reduction in *DND1* expression was detected in the *DND1* silenced lines (Fig. 1).

Mutation in *DND1* increases the SA content in *A. thaliana*³. To test whether this is also the case in the potato, the SA concentration of leaves of in vitro-grown *DND1* silenced plants was measured and compared to that of the control DES. A tremendous increase in SA concentration was detected in each *DND1* line; while the SA content of DES was $127 \pm 18 \text{ ng g}^{-1}$ fresh weight (FW), it was elevated to 2723 ± 1093 , 1178 ± 782 , and $1333 \pm 416 \text{ ng g}^{-1}$ FW in DND1-5, DND1-8, and DND1-17, respectively (Fig. 2). In addition to SA, the phytohormones jasmonic acid (JA) and abscisic acid (ABA) regulate plant defenses through synergistic and antagonistic actions¹⁴. An elevated level of JA and its leucine conjugate was detected in the leaves of *DND1* silenced plants (Fig. 2). In contrast, no alteration in ABA level was observed in *DND1* lines (Supplementary Fig. 1).

Since secondary metabolites, especially those synthesized in the phenylpropanoid pathway, have an important role in plant defense against pathogens¹⁵, a targeted metabolite analysis of potato leaves extending to nine compounds was performed. An increased level of chlorogenic acid and its derivatives, as well as that of *para*-hydroxybenzoic acid, was found in *DND1* silenced lines, whereas the concentrations of taxifolin and rutin were decreased (Fig. 2). The silencing did not influence the levels of dihydrokaempferol, phaseic acid, and dihydrophaseic acid (Supplementary Fig. 1).

Transcriptome analysis of the *DND1* silenced potato lines

Transcriptome analysis was performed to understand the influence of *DND1* silencing on gene expression. RNA was isolated from the leaves of in vitro-grown plants in two biological replicates. The RNA-seq produced

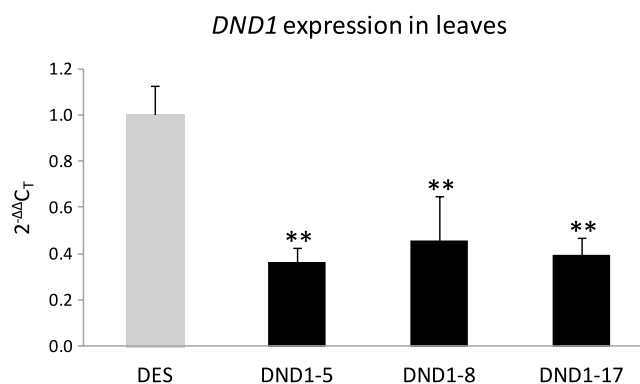


Fig. 1. Level of *DND1* expression in *DND1* silenced lines DND1-5, DND1-8 and DND1-17 compared to the non-transformed control 'Désirée' (DES). RNA was isolated from the middle leaves of in vitro plants; three leaves/plants were harvested from three plants/lines. The RT-qPCR analysis was carried out using the *EF1α* as a reference gene. The Y-axis shows the average relative $2^{-\Delta\Delta C_T}$ values compared to the average $2^{-\Delta\Delta C_T}$ value of DES set as 1.0. The averages were calculated from three technical replicates. The standard deviations are indicated by the error bars. Significant differences between the *DND1* silenced lines and DES were determined by Student's *t*-test and labelled by ** ($p < 0.01$).

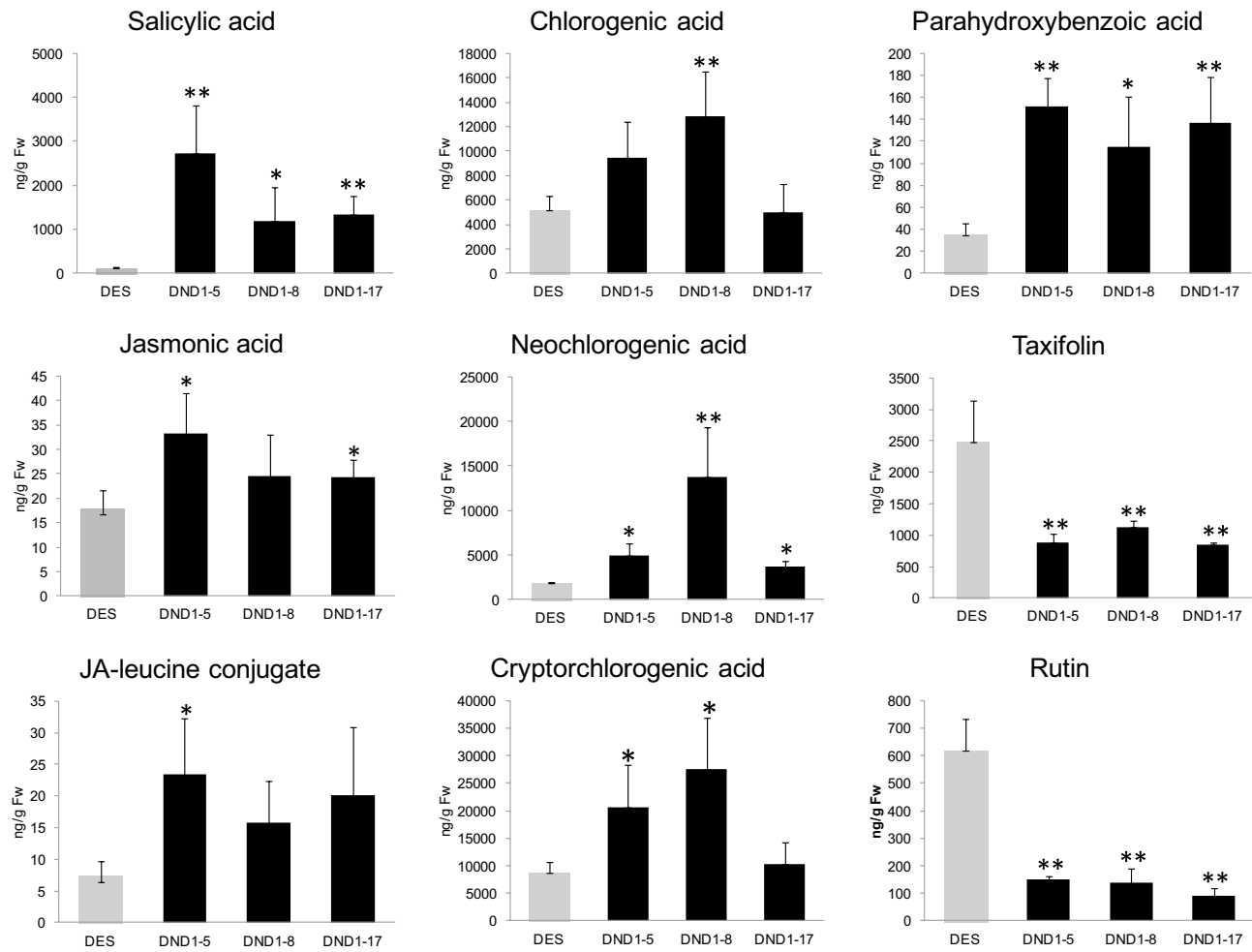


Fig. 2. Concentration differences of selected hormones and secondary metabolites between the non-transformed control ‘Désirée’ (DES) and the *DND1* silenced lines DND1-5, DND1-8 and DND1-17. The data were obtained from four biological replicates from the leaves of each line. Each biological replicate contained the leaves of five *in vitro* plants. The standard deviations are indicated by the error bars. Significant differences between the *DND1* silenced lines and DES were determined by Student’s *t*-test and labelled by * ($p < 0.05$) and ** ($p < 0.01$).

good-quality data (Supplementary Table 1), resulting in close to 90% of total and unique mapped reads. The correlation coefficients between the two biological replicates varied from 0.97 to 0.99 overall (Supplementary Table 2). Expression of 18,752 genes was detected in all samples (Fig. 3a). The number of differentially expressed genes (DEGs) compared to DES (Supplementary Tables 3–5) was very similar in DND1-8 (1629 up, 1608 down) and DND1-17 (1744 up, 1347 down), while it was a bit higher in DND1-5 (2146 up, 1847 down). Data are visualized with bar graphs in Fig. 3b and with volcano plots in Supplementary Fig. 2. The number of common genes upregulated in each *DND1* silenced line was 1138 (Fig. 3b), whereas the number of downregulated genes was 728 (Fig. 3c).

Gene ontology (GO) analysis revealed 57 significantly altered terms: 31 biological processes, 23 molecular functions, and three cellular components. The highest number of genes belonged to the “catalytic activity,” “membrane,” “ion binding,” “response to stimulus,” and “small molecule binding” categories. Interestingly, only five out of 57 categories showed downregulation, namely, “response to chemical,” “response to organic substance,” “cellular response to organic substance,” “cellular response to endogenous stimulus,” and “trehalose metabolism in response to stress” (Fig. 4).

Kyoto Encyclopedia of Genes and Genomes (KEGG)¹⁶ analysis was used to further refine the DEG categories by sorting the genes into different metabolic pathways (Fig. 5, Supplementary Tables 6 and 7). It was found that the greatest changes occurred in carbohydrate, lipid, and amino acid metabolism followed by the biosynthesis of other secondary metabolites. For example, *β*-FRUCTOFURANOSIDASE CELL WALL ISOZYME, SUCROSE SYNTHASE, different types of CHITINASES, PECTATE LYASE, GLUTAMATE DECARBOXYLASE, FATTY ACID DESATURASE, LIPOXYGENASE, GLUTAMATE DECARBOXYLASE, ASPARTATE AMINOTRANSFERASE, and a large number of GLUTATHIONE TRANSFERASES were highly activated. While the number of upregulated and downregulated genes was similar in carbohydrate, lipid, and amino acid metabolism, the extent of changes was, in general, less in the repressed genes than in the activated genes. In the secondary metabolite category, upregulation was the dominant tendency; 41 genes involved in secondary metabolite synthesis, including

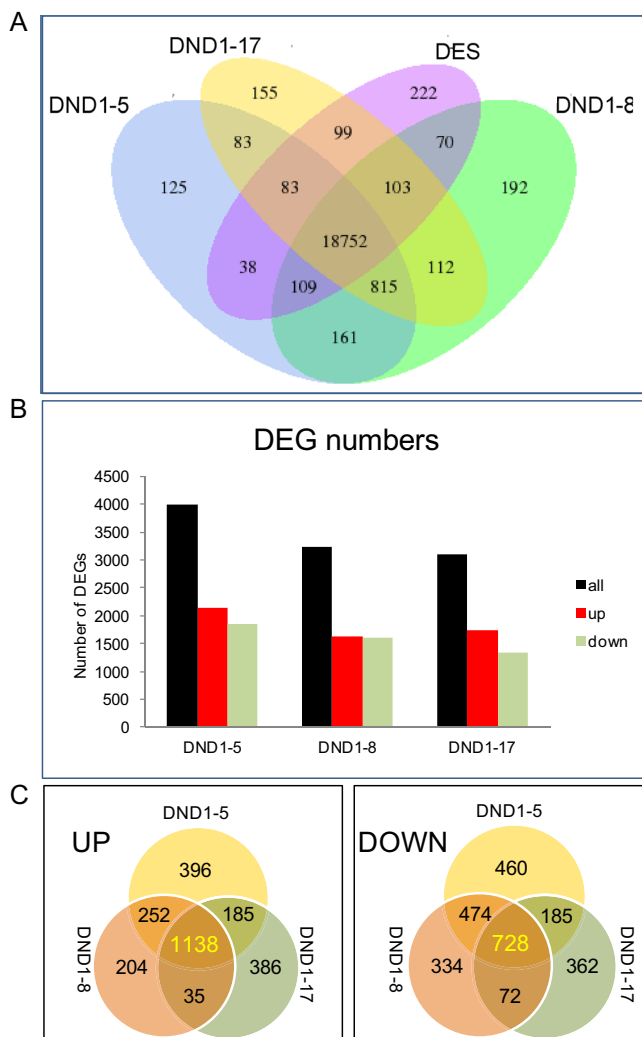


Fig. 3. The number of unigenes (A) and differentially expressed genes (DEGs) (B,C) in the leaves of the non-transformed control ‘Désirée’ (DES) and the *DND1* silenced lines DND1-5, DND1-8 and DND1-17. (B) The number of up- and downregulated DEGs in the *DND1* silenced lines as compared to DES. (C) Venn diagram of up- and downregulated DEGs. The overlaps represent the genes differentially expressed in more than one line. The number of DEGs detected in each *DND1* silenced line is highlighted in yellow.

ELICITOR-INDUCIBLE CYTOCHROME P450, *GLYCOSYLTRANSFERASES*, *PHENYLALANINE LYASES*, and *LEUCOANTHOCYANIDIN DIOXYGENASE*, were upregulated, and only ten genes were downregulated. This tendency was similar to the genes encoding proteins functioning in environmental adaptation (45 up and 11 down). The level of expression of genes encoding *CYSTEINE PROTEASE*, *PATHOGENESIS RELATED PROTEINS*, *HEAT SHOCK PROTEINS*, and *CALCIUM-BINDING EF HAND FAMILY PROTEINS* was significantly increased. Furthermore, substantial changes were detected in the expression level of genes involved in signal transduction related to environmental information processing; 42 genes were upregulated, and 35 genes were downregulated. Several genes related to auxin response (e.g., *AUXIN-RESPONSIVE PROTEIN*, *AUXIN-RESPONSE FACTOR*) and ethylene sensitivity (e.g., *ETHYLENE-INSENSITIVE3-LIKE 1, 2, and 3*) were repressed.

Protein–protein interaction network prediction

Interactions of potato proteins can be predicted based on the STRING database. To do so, the identified potato protein sequences were downloaded from the STRING database, and SpudDB identifiers and sequences were assigned to them. From the common DEG list of the DND1 lines containing 1866 genes in total, 325 corresponding proteins (nodes) with 468 connections (edges) were identified; of them, 230 proteins with 381 connections are found in the largest connected cluster (Fig. 6 and Supplementary Table 8). Within this cluster, several centrals can be found with the most interacting proteins and their primary neighbours. These central proteins possess very diverse functions, including histones, kinases, ubiquitin family proteins, heat shock proteins, and brassinosteroid signalling pathway proteins.

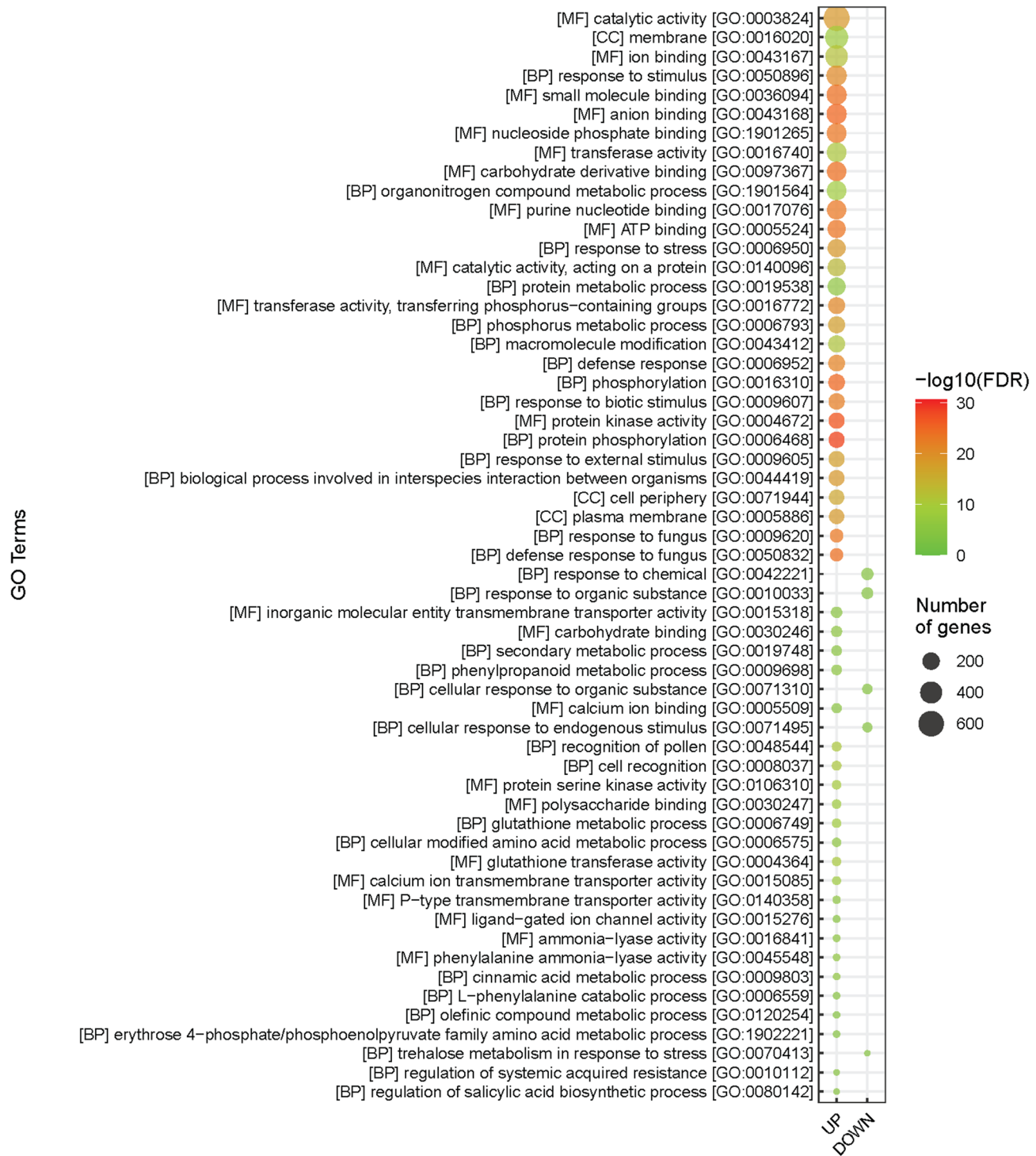


Fig. 4. Bubble plot diagram of the significantly (Benjamini and Hochberg FDR correction: $p \leq 0.0001$ and REVIGO: simrel 0.7) up- and downregulated GO terms common in the *DND1* silenced lines DND1-5, DND1-8, and DND1-17 compared to the non-transformed control 'Désirée'. BP, biological process; CC, cellular component; MF, molecular function; FDR, false discovery rate.

Transcription factors differentially expressed in the *DND1* silenced potato lines

Since transcription factors (TFs) are key regulators of stress responses, differentially expressed TFs were analyzed first. Of the TFs that were differentially expressed in each *DND1* silenced line, we identified 60 upregulated and 63 downregulated genes (Fig. 7). The WRKY family genes (WRKY6, 13, 16, 24, 30, 40, 41, 48, 51, 54, 70, 75) dominated the group of upregulated genes with the highest increase in expression of WRKY40 (average log₂ fold change: 9.9). Several members of the NAC TF family (NAC008, 31, 35, 42, 73, 82, 86, 90) and bHLH TF genes (bHLH13, 29, 35, 90) were also present in the upregulated group. The group of downregulated genes

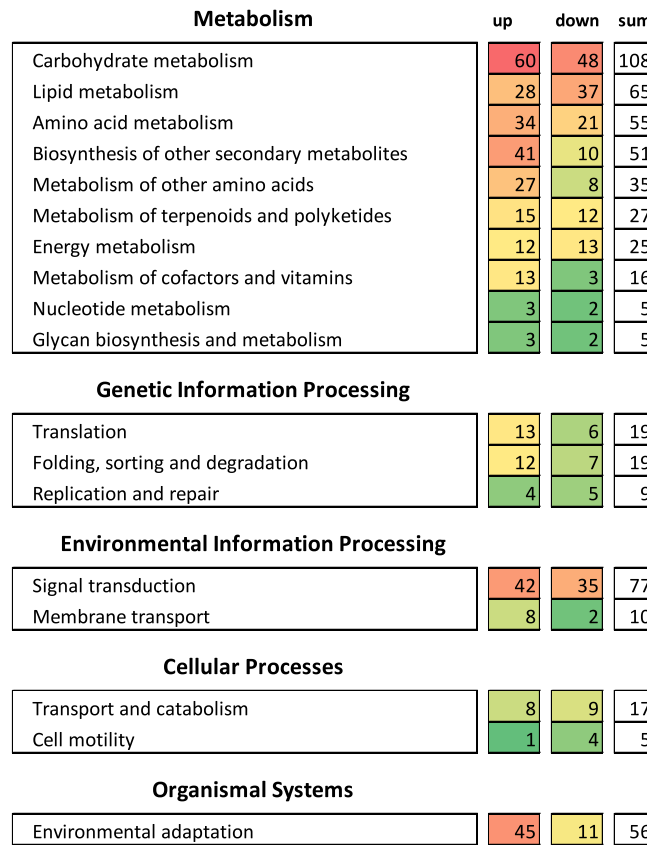


Fig. 5. KEGG pathways¹⁶ significantly enriched in each *DND1* silenced line. The number of up- and downregulated genes belonging to the identified pathways is indicated. Colours from green to red correlate with the number of genes between 1 and 60.

was dominated by the genes encoding bHLH TFs (*bHLH8*, 50, 51, 58, 63, 93, 104, 121, 130, 137, 151), out of which *bHLH8*, 151 and 63 had the strongest repression, with average log₂ fold changes of -3.6, -3.4, and -2.2, respectively.

Pathogenesis-related genes differentially expressed in the *DND1* silenced potato lines

With the exception of three slightly downregulated pathogenesis-related genes, all of the others were upregulated (Fig. 8). Sixteen categories of upregulated genes could be established. Most of them were related to fungal resistance/sensitivity against, e.g., leaf rust (*LRK10Ls*, *Lr10s*), powdery mildew (*Mlos*), downy mildew (*DMR6s*), and late blight (*R1Bs*). Several pathogenesis-related protein genes (*PRPs*), as well as other disease resistance protein genes (*RP*s) or probable disease resistance protein genes and hypersensitivity-related protein genes (*HSRs*), were also upregulated. Additionally, several alleles of the gene encoding the TMV resistance protein N were expressed at a higher level in the leaves of *DND1* silenced plants than in DES leaves.

Validation of RNA-seq results

Transcriptome data were validated via RT-qPCR analysis of three upregulated and three downregulated genes. The upregulated genes tested were the TFs *WRKY40* and *NAC90* and the powdery mildew resistance gene *MLO-LIKE PROTEIN 6* (*MLO6*). The downregulated genes tested were *14 kD PROLINE-RICH PROTEIN (PRO)*, *NADH NITRATE REDUCTASE 3* (*NR3*), and the TF *bHLH8*. The expression trends of the genes using RNA-seq and RT-qPCR were similar in each *DND1* line. Further, the correlation coefficients of $R^2 = 0.6878$ in *DND1-5*, $R^2 = 0.9466$ in *DND1-8*, and $R^2 = 0.9026$ in *DND1-17* confirmed the reliability of the transcriptome data (Fig. 9).

Effect of exogenous SA on the expression of selected genes

SA is a hormone molecule that can be found at a wide range of endogenous levels in plants and induces responses to various stresses¹⁷. In *A. thaliana*, SA induces the expression of *WRKY40*¹⁸, *PR1*¹⁹, *MLO6*²⁰, and *DMR6*²¹; these genes were highly expressed in the *DND1* silenced lines with high SA content. Although no data on the SA-triggered *NAC90* transcription activation was found in the literature, this TF was also highly expressed in all three *DND1* lines (Fig. 7). To test whether SA can also activate the expression of these genes in the potato, the foliage of greenhouse-grown DES plants was sprayed with SA solution, and leaf samples were collected 24 h after

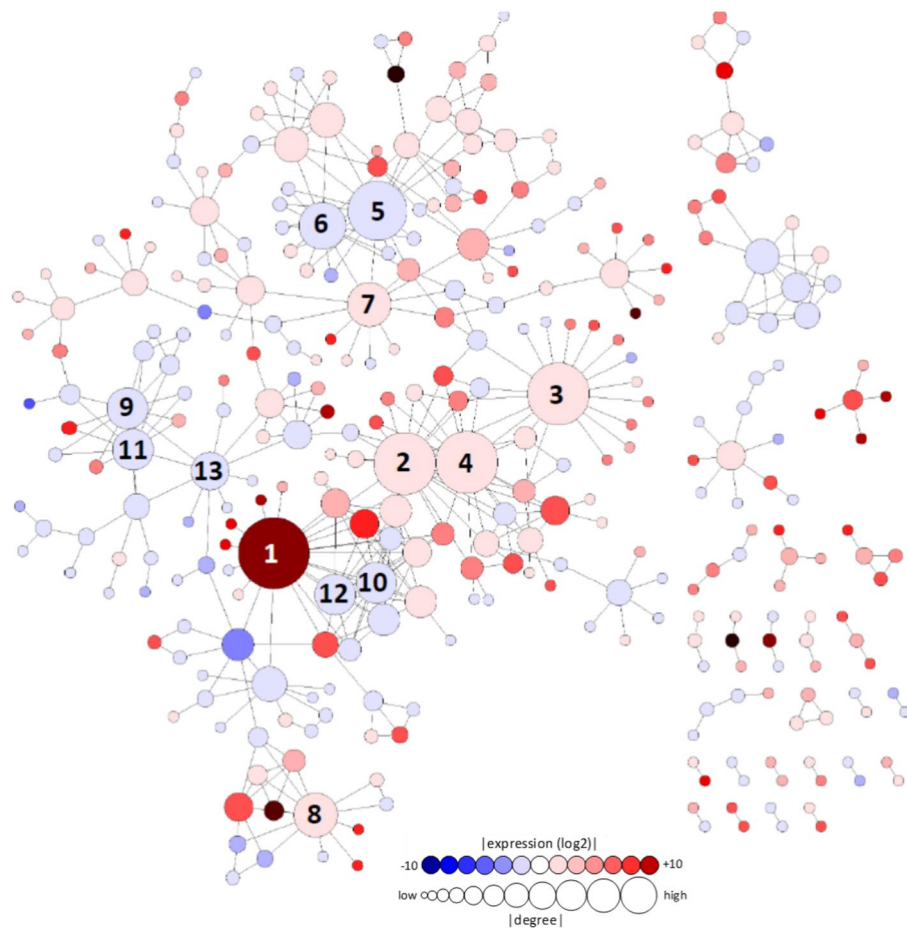


Fig. 6. Predicted interactions between potato proteins encoded by differentially expressed genes in *DND1* silenced lines. The colour of the circles is associated with gene expression (log₂ fold change), while their diameter is correlated with the number of connections. The interacting network contains 325 nodes and 468 edges. Nodes with at least ten connections are numbered, namely: (1) Soltu.DM.01G021410 [histone H3.2-like], (2) Soltu.DM.03G012070 [polyubiquitin-like], (3) Soltu.DM.03G025860 [protein NBR1 homolog], (4) Soltu.DM.03G012080 [polyubiquitin-like], (5) Soltu.DM.10G020640 [heat shock cognate 70 kDa protein 2], (6) Soltu.DM.09G002330 [heat shock cognate 70 kDa protein 2-like], (7) Soltu.DM.03G023440 [heat shock protein 83], (8) Soltu.DM.05G025830 [probable small nuclear ribonucleoprotein G], (9) Soltu.DM.12G005470 [BRASSINAZOLE-RESISTANT 1-like], (10) Soltu.DM.12G022120 [histone H2A.6-like], (11) Soltu.DM.04G034930 [BRASSINAZOLE-RESISTANT 1-like], (12) Soltu.DM.01G039150 [histone H2A.1], (13) Soltu.DM.12G007030 [cryptochrome-1-like]. The source code (graphml) of the graphs is deposited into GitHub Gist and accessible online via yEd Live (<https://bit.ly/3tLMqbH>).

treatment. RT-qPCR analysis showed that all five selected genes (*WRKY40*, *NAC90*, *PR1*, *MLO6*, and *DMR6*) were strongly SA-inducible (Fig. 10).

Discussion

Previously, it was shown that the silencing of *DND1* leads to resistance to late blight, powdery mildew, and gray mold diseases^{11,12}. Using the same lines tested earlier for fungal resistance, our experiment detected an approximately 10- to 20-fold increase in the SA concentration in leaves; this is in good agreement with the 15-fold increase detected in *dnd1* mutant *Arabidopsis* plants³. It is generally considered that SA participates in activating of plant defense mechanisms and acts with other signalling molecules, such as JA²². Besides the elevation of SA content, a 1.5- to 2.0-fold increase in JA and JA-Leu conjugate levels was also observed in the *DND1* silenced lines. JA, along with its conjugated forms, tunes plant defense mechanisms by regulating the expression of JA-associated genes imparting the resistance phenotype²³. It was demonstrated that JA-Leu can serve as a ligand to promote the interaction between CORONATINE INSENSITIVE1 (COI1) and JASMONATE-ZIM (Zinc-finger Inflorescence Meristem) domain (JAZ) repressor proteins inducing JAZ's degradation²⁴.

SA- and JA-driven elicitation of secondary metabolites, including phenolics and flavonoids, was detected in various plant species²⁵. In line with this general observation, elevations of concentrations of chlorogenic acid (ester of caffeic acid and quinic acid) and its derivatives were detected in the leaves of *DND1* silenced lines compared to the control DES. Thus, the demonstrated antimicrobial effect of chlorogenic acid and related

UP		Foldchange log2					Foldchange log2					DOWN	
Gene ID	TFs	DND1-5	DND1-8	DND1-15		DND1-5	DND1-8	DND1-17	TFs	Gene ID			
Soltu.DM.08G015910	WRKY40	10.02494	10.16561	9.514786		-0.49552	-0.6135	-0.53951	EFM	Soltu.DM.04G002320			
Soltu.DM.12G012040	SARD1	8.886965	8.686913	8.092008		-0.53263	-0.66802	-0.55677	AN11-A	Soltu.DM.01G025100			
Soltu.DM.05G010910	bHLH35	8.508768	8.276044	8.386892		-0.52405	-0.63769	-0.61181	C2A9.03	Soltu.DM.03G004150			
Soltu.DM.05G016710	NAC042	8.079079	7.993906	6.977055		-0.74293	-0.55718	-0.48269	RAP2-4	Soltu.DM.12G001810			
Soltu.DM.08G015900	WRKY40	7.341952	7.109429	7.035427		-0.66591	-0.73414	-0.43514	GA1	Soltu.DM.07G028300			
Soltu.DM.08G012710	WRKY51	7.307496	7.049477	7.019083		-0.58986	-0.64265	-0.64733	bHLH104	Soltu.DM.09G005350			
Soltu.DM.10G019280	DREB2A	7.036311	7.123872	6.83883		-0.62508	-0.58299	-0.71598	RAP2-2	Soltu.DM.06G009770			
Soltu.DM.12G007400	WRKY51	6.849336	7.331328	6.59172		-0.59569	-0.66671	-0.66276	bHLH130	Soltu.DM.08G004720			
Soltu.DM.04G028130	MYB4	7.050359	6.743849	6.036357		-0.75128	-0.5853	-0.59542	ERF4	Soltu.DM.03G033840			
Soltu.DM.10G019290	WRKY51	6.600134	6.443461	6.370687		-0.66665	-0.63766	-0.64407	STOP1	Soltu.DM.06G030160			
Soltu.DM.03G014050	DREB2A	6.562165	6.204421	5.9714		-0.80461	-0.67404	-0.53399	IAA22	Soltu.DM.05G022080			
Soltu.DM.06G031190	ZAT11	5.844906	5.679262	5.699636		-0.70676	-0.58858	-0.71875	SCL1	Soltu.DM.02G016980			
Soltu.DM.04G023540	WRKY51	5.865984	5.726295	5.424949		-0.69533	-0.62729	-0.71809	EARLY FLOWR	Soltu.DM.07G027240			
Soltu.DM.11G022040	WRKY48	5.441142	5.384892	5.002596		-0.51707	-0.97306	-0.6121	AS2-like 39	Soltu.DM.05G022060			
Soltu.DM.05G023360	NAC090	5.074313	5.199524	5.18982		-0.87985	-0.55208	-0.72307	ERF4	Soltu.DM.06G014070			
Soltu.DM.06G005360	AS2-like 7	4.901346	4.730974	4.848173		-0.78539	-0.68515	-0.7223	EIN3	Soltu.DM.08G011110			
Soltu.DM.08G022950	NAC086	4.837249	4.870469	4.601245		-0.90175	-0.64476	-0.70841	ERF4	Soltu.DM.09G006830			
Soltu.DM.10G021890	GT-3a	4.656846	4.730162	4.122957		-0.79082	-0.88663	-0.61963	COL6	Soltu.DM.04G031540			
Soltu.DM.10G019380	WRKY70	4.489063	4.216154	4.221509		-0.57371	-0.84463	-0.70721	DOF1.7	Soltu.DM.01G051040			
Soltu.DM.09G007650	MYB	4.152893	4.403976	4.032462		-0.99295	-0.8449	-0.47272	HAT4	Soltu.DM.05G022070			
Soltu.DM.10G017860	NAC035	4.405575	4.015473	4.047871		-0.55119	-0.79394	-0.96602	TCP22	Soltu.DM.12G003910			
Soltu.DM.05G025220	ZAT11	4.087903	4.102712	3.921943		-0.82977	-0.64601	-0.84251	BE51	Soltu.DM.02G006490			
Soltu.DM.06G009320	SARD1	3.422883	3.360623	2.756785		-0.17092	-0.73056	-0.5823	SZF2	Soltu.DM.04G001380			
Soltu.DM.03G033680	NAC031	3.172098	2.91944	3.152371		-0.77763	-0.79711	-0.82597	EIN3	Soltu.DM.01G007500			
Soltu.DM.06G001380	ZAT11	3.232179	3.294297	2.526513		-0.10294	-0.79789	-0.6896	ERF5	Soltu.DM.07G013320			
Soltu.DM.06G031200	ZAT11	2.865578	3.322166	2.624454		-0.91191	-0.84436	-0.75538	bHLH121	Soltu.DM.05G005300			
Soltu.DM.10G020840	bHLH29	3.084749	2.458369	3.208298		-0.87374	-0.7595	-0.8844	EIN3	Soltu.DM.03G019670			
Soltu.DM.11G026530	NAC008	2.952655	2.825107	2.573553		-0.96996	-0.81154	-0.73798	ARF7A	Soltu.DM.10G002110			
Soltu.DM.02G033440	MYB113	2.931655	2.395099	2.957687		-0.63585	-0.75074	-1.14788	CBP1	Soltu.DM.05G002670			
Soltu.DM.02G029480	AIL6	2.351767	2.870296	2.642251		-0.72578	-0.83351	-0.99028	COL16	Soltu.DM.01G049490			
Soltu.DM.05G021130	MYB108	2.746479	2.530176	2.350989		-0.98264	-1.1517	-0.5133	UNE10	Soltu.DM.06G011430			
Soltu.DM.05G008840	bHLH90	2.778863	2.532275	2.30454		-1.13398	-0.8263	-0.75289	CYCLOIDEA	Soltu.DM.04G036140			
Soltu.DM.11G025600	LET12	2.740794	2.530176	2.28992		-1.05852	-0.79901	-0.87858	DUVARICATA	Soltu.DM.04G033390			
Soltu.DM.05G012130	WRKY75	2.410109	2.525211	2.525211		-0.86628	-1.19592	-0.75898	ERF010	Soltu.DM.05G022630			
Soltu.DM.11G026510	ZAT11	2.39519	2.968985	2.072419		-0.98069	-0.91866	-0.92518	BBX21	Soltu.DM.03G034300			
Soltu.DM.03G013350	WRKY70	2.68571	2.288743	2.404044		-0.99752	-0.78329	-1.05759	RF2b	Soltu.DM.01G031430			
Soltu.DM.05G023310	WRKY54	2.393996	2.230248	2.144359		-0.98641	-0.87731	-0.9866	bHLH63	Soltu.DM.05G003170			
Soltu.DM.12G027800	DOF3.1	2.087313	1.907859	2.66976		-0.94561	-1.06426	-0.88298	EFM	Soltu.DM.01G048600			
Soltu.DM.09G011140	ZAT9	2.42108	2.37994	1.89059		-0.95948	-0.80852	-1.17623	COL11	Soltu.DM.07G006060			
Soltu.DM.10G005570	WRKY30	2.279863	2.024591	1.979244		-1.19388	-0.75634	-1.05337	bHLH137	Soltu.DM.01G035980			
Soltu.DM.02G017000	AS2-like 8	1.638112	1.894108	2.512349		-1.15704	-1.04383	-0.91401	ANAC029	Soltu.DM.01G050710			
Soltu.DM.01G031470	WRKY41	1.873603	2.407587	1.69075		-0.80744	-1.03561	-1.27678	SAUR72	Soltu.DM.10G001250			
Soltu.DM.02G020430	NAC073	2.218187	1.830703	1.740117		-1.24199	-1.07402	-0.84506	ANAC083	Soltu.DM.06G029100			
Soltu.DM.05G005130	WRKY6	1.957742	1.957167	1.683868		-1.04946	-0.77579	-1.35955	RAV1	Soltu.DM.05G022590			
Soltu.DM.05G020000	PHL8/MYB	1.259546	2.532275	1.682557		-1.23159	-1.21412	-0.81731	bHLH58	Soltu.DM.02G006820			
Soltu.DM.08G005640	bHLH13	1.308309	1.412497	2.303159		-1.25579	-1.39647	-0.71802	COL4	Soltu.DM.11G012310			
Soltu.DM.09G009490	WRKY24	1.629067	1.655013	1.09003		-1.36918	-1.12433	-0.97645	EREBP4	Soltu.DM.06G018130			
Soltu.DM.03G022590	CO3	1.308387	1.071034	1.320915		-1.11738	-1.33187	-1.23081	MYB308	Soltu.DM.06G022770			
Soltu.DM.04G035890	BEL1-like 3	1.010793	1.115527	1.286282		-1.07119	-1.22919	-1.38054	bHLH93	Soltu.DM.03G034030			
Soltu.DM.02G004200	WRKY6	1.386411	1.059997	0.913511		-1.20082	-1.51242	-0.98763	MYB36	Soltu.DM.08G024170			
Soltu.DM.06G020280	TCP8	1.232681	1.102922	0.972365		-0.9858	-0.6301	-2.12114	IAA11	Soltu.DM.01G006210			
Soltu.DM.08G014820	ATHB-15	1.081107	1.060318	1.099838		-1.45882	-1.5335	-0.79643	ATHB-7	Soltu.DM.07G020090			
Soltu.DM.11G008090	NAC082	1.405764	1.091992	1.723874		-1.40443	-1.58156	-0.87467	ERF106	Soltu.DM.02G027820			
Soltu.DM.11G010580	WRKY16	0.927173	1.112856	0.859759		-1.18661	-1.52192	-1.17254	NF-YB-3	Soltu.DM.08G014030			
Soltu.DM.05G019990	WRKY41	1.023461	0.910057	0.945132		-1.18724	-1.07681	-1.66254	ATHB-52	Soltu.DM.04G025540			
Soltu.DM.05G024540	SCL13	1.099495	0.882863	0.864442		-1.02724	-1.38862	-1.62307	ERF2	Soltu.DM.07G013020			
Soltu.DM.08G001050	GATA26	0.800441	0.869643	1.042301		-1.4243	-1.83655	-0.99621	ZAT5	Soltu.DM.11G010110			
Soltu.DM.01G027400	NF-YA-9	0.930462	0.979371	0.573188		-1.28053	-1.37663	-1.63974	bHLH50	Soltu.DM.03G014560			
Soltu.DM.12G010270	ATHB-15	0.664227	0.837657	0.764529		-1.30011	-1.50602	-1.52105	ERF061	Soltu.DM.01G027830			
Soltu.DM.10G005290	GIF3	0.582077	0.693616	0.570773		-2.12805	-1.44946	-1.59679	bHLH51	Soltu.DM.06G022200			

Fig. 7. Differentially expressed transcription factors (TFs) in the leaves of the *DND1* silenced lines DND1-5, DND1-8 and DND1-17 compared to the non-transformed control 'Désirée' leaves. The intensity of colours indicates the degree of the difference (log2 fold change).

compounds²⁶ may contribute to the fungal resistance of DND1 lines. In contrast, the concentration of the flavonoid taxifolin (also known as dihydroquercetin) and the flavonoid glycoside rutin were lower in DND1

Foldchange log2					
UP	Gene ID	DND1-5	DND1-8	DND1-17	Gene description
Soltu.DM.12G011950	4.339971	3.916491	3.696752	Leaf rust 10 disease-resistance locus receptor-like protein kinase-like 2.1; LRK10L-2.1	
Soltu.DM.02G026090	3.988425	4.090293	3.074321	Leaf rust 10 disease-resistance locus receptor-like protein kinase-like 2.1; LRK10L-2.1	
Soltu.DM.12G011930	3.40072	3.492737	3.120173	Leaf rust 10 disease-resistance locus receptor-like protein kinase-like 1.2; LRK10L-1.2	
Soltu.DM.05G003740	3.28678	3.224833	2.198471	Leaf rust 10 disease-resistance locus receptor-like protein kinase-like 1.1; LRK10L-1.1	
Soltu.DM.02G026160	3.0642	2.931651	1.849134	Leaf rust 10 disease-resistance locus receptor-like protein kinase-like 1.4; LRK10L-1.4	
Soltu.DM.02G026170	2.447525	2.947751	2.35515	Leaf rust 10 disease-resistance locus receptor-like protein kinase-like 1.2; LRK10L-1.2	
Soltu.DM.03G033670	1.733086	1.738377	1.303695	Leaf rust 10 disease-resistance locus receptor-like protein kinase-like 1.2; LRK10L-1.2	
Soltu.DM.05G003720	1.407678	1.330804	1.212192	Leaf rust 10 disease-resistance locus receptor-like protein kinase-like 1.1; LRK10L-1.1	
Soltu.DM.12G011910	1.39948	1.477312	1.05606	Leaf rust 10 disease-resistance locus receptor-like protein kinase-like 2.1; LRK10L-2.1	
Soltu.DM.05G003790	1.300558	1.180279	1.31678	Leaf rust 10 disease-resistance locus receptor-like protein kinase-like 1.1; LRK10L-1.1	
Soltu.DM.05G003560	1.194093	1.07435	1.03661	Leaf rust 10 disease-resistance locus receptor-like protein kinase-like 2.8; LRK10L-2.8	
Soltu.DM.11G005620	1.045786	0.860052	1.115551	Leaf rust 10 disease-resistance locus receptor-like protein kinase-like 2.1; LRK10L-2.1	
Soltu.DM.01G004790	4.640869	4.364631	4.635413	Rust resistance kinase Lr10	
Soltu.DM.01G004780	2.543801	2.815214	2.594284	Rust resistance kinase Lr10	
Soltu.DM.01G004700	2.649098	2.578762	2.633239	Rust resistance kinase Lr10	
Soltu.DM.01G004970	2.215669	2.329707	2.47361	Rust resistance kinase Lr10	
Soltu.DM.01G005070	2.158699	2.33518	1.791995	Rust resistance kinase Lr10	
Soltu.DM.01G004860	1.653599	1.534226	1.570908	Rust resistance kinase Lr10	
Soltu.DM.01G004830	1.463698	1.685339	1.555108	Rust resistance kinase Lr10	
Soltu.DM.02G021320	2.263508	2.211728	2.122219	Rust resistance kinase Lr10	
Soltu.DM.11G005850	1.284292	1.126095	1.323038	Rust resistance kinase Lr10	
Soltu.DM.11G022590	8.186382	7.474116	7.091215	MLO-like protein 6; Mlo6	
Soltu.DM.03G013460	5.334547	5.061854	5.15902	MLO-like protein 6; Mlo6	
Soltu.DM.06G005820	4.391293	4.311826	3.580096	MLO-like protein 6; Mlo6	
Soltu.DM.08G006400	0.983489	0.940353	0.77502	MLO-like protein 1; Mlo1	
Soltu.DM.07G024430	0.682569	0.603118	0.645637	MLO-like protein 11; Mlo11	
Soltu.DM.06G028410	4.996631	4.641426	4.880414	Downy mildew resistance 6; DMR6	
Soltu.DM.03G021450	2.16173	1.535132	1.774638	Downy mildew resistance 6; DMR6	
Soltu.DM.05G005400	1.615592	1.079791	1.271573	Putative late blight resistance protein homolog R1C-3	
Soltu.DM.01G000440	1.074476	1.177471	0.940943	Putative late blight resistance protein homolog R1B-8	
Soltu.DM.10G004030	1.032494	1.091421	0.945729	Putative late blight resistance protein homolog R1B-14	
Soltu.DM.11G007400	0.874254	1.086637	0.874899	Putative late blight resistance protein homolog R1B-12	
Soltu.DM.01G045900	9.708726	9.964642	9.827016	Pathogenesis-related protein 1; PR-1	
Soltu.DM.10G014420	7.917204	8.551285	7.199485	Pathogenesis-related protein 1C	
Soltu.DM.09G007060	8.563899	7.230198	7.305747	Pathogenesis-related leaf protein 4; P4	
Soltu.DM.10G014400	6.266903	6.903001	6.592671	Pathogenesis-related protein 1C	
Soltu.DM.09G007020	6.601566	5.502125	5.644384	Pathogenesis-related leaf protein 4; P4	
Soltu.DM.09G007030	6.456653	5.224666	5.54371	Pathogenesis-related leaf protein 6; P6	
Soltu.DM.12G007830	3.994032	3.92965	4.124165	Pathogenesis-related protein R major form	
Soltu.DM.12G007860	4.235905	3.963545	3.383693	Pathogenesis-related protein R major form	
Soltu.DM.01G036420	3.153596	3.321786	3.031463	Pathogenesis-related protein P2	
Soltu.DM.09G027700	1.551817	1.408992	1.419377	Pathogenesis-related protein STH-2	
Soltu.DM.02G016660	2.872371	2.673967	2.034153	Pathogenesis-related genes transcriptional activator PTI5	
Soltu.DM.01G034620	2.458132	2.479239	2.172102	Pathogenesis-related genes transcriptional activator PTI6	
Soltu.DM.04G026010	2.654015	3.03651	2.45036	Pathogen-related protein	
Soltu.DM.04G026000	1.04681	0.983425	0.976372	Pathogen-related protein	
Soltu.DM.10G016700	2.175044	2.065206	2.45461	Disease resistance protein RPM1	
Soltu.DM.08G000720	2.254739	2.216188	2.223705	Disease resistance protein At4g27190	
Soltu.DM.12G022840	1.70114	1.282595	1.658408	Disease resistance protein RP55	
Soltu.DM.01G031090	1.555496	1.483741	1.349965	Disease resistance RPP8-like protein 3	
Soltu.DM.04G006280	1.206644	1.084225	1.212407	Disease resistance protein RPP13	
Soltu.DM.01G041640	1.322947	1.148809	0.952562	Disease resistance protein RPS4	
Soltu.DM.04G010740	0.865113	0.838566	0.739278	Disease resistance protein RGA2	
Soltu.DM.10G022090	3.09419	2.992191	3.125566	Putative disease resistance protein RGA3	
Soltu.DM.08G021030	2.408713	3.015277	2.7113831	Putative disease resistance protein RGA4	
Soltu.DM.08G020500	2.234957	2.26687	2.319256	Putative disease resistance protein RGA1	
Soltu.DM.08G021040	2.255469	2.330204	2.233918	Putative disease resistance protein RGA1	
Soltu.DM.09G008160	1.469715	1.451923	1.500016	Putative disease resistance protein RGA1	
Soltu.DM.10G006190	1.17339	1.091066	1.203942	Putative disease resistance protein RGA4	
Soltu.DM.10G016590	1.083939	1.194274	1.043277	Putative disease resistance protein RGA4	
Soltu.DM.10G016640	0.978214	1.144849	0.992298	Putative disease resistance protein RGA4	

Fig. 8. (continued)

Soltu.DM.04G008210	4.132579	3.7929	3.767564	Putative disease resistance protein At1g50180
Soltu.DM.12G003390	1.852005	1.882991	2.417893	Probable disease resistance RPP8-like protein 2
Soltu.DM.12G004760	1.92193	2.012902	1.13307	Putative disease resistance RPP13-like protein 2
Soltu.DM.09G029420	1.675185	1.622851	1.36688	Putative disease resistance protein At4g11170
Soltu.DM.04G000760	1.47608	1.446302	0.943412	Probable disease resistance protein At1g61180
Soltu.DM.02G029370	1.315262	1.14299	0.968906	Probable disease resistance protein At5g66900
Soltu.DM.02G029390	1.152329	1.095801	0.84655	Probable disease resistance protein At5g66900
Soltu.DM.02G029390	1.152329	1.095801	0.84655	Probable disease resistance protein At5g66900
Soltu.DM.02G029410	1.102622	1.020114	0.794845	Probable disease resistance protein At4g33300
Soltu.DM.02G029410	1.102622	1.020114	0.794845	Probable disease resistance protein At4g33300
Soltu.DM.03G003930	5.152857	5.422546	4.64759	Hyper-sensitivity-related 4; HSR4
Soltu.DM.03G003940	5.009119	4.966742	4.510044	Hyper-sensitivity-related 4; HSR4
Soltu.DM.03G003950	3.92035	3.932615	3.676045	Hyper-sensitivity-related 4; HSR4
Soltu.DM.03G027120	2.519742	2.347985	1.933304	Hypersensitive-induced response protein 1; HIR1
Soltu.DM.03G004080	1.224238	1.527645	0.999615	Hyper-sensitivity-related 4; HSR4
Soltu.DM.06G026180	1.219239	0.867952	0.900865	Hypersensitive-induced response protein 1; HIR1
Soltu.DM.01G001880	2.57895	2.499585	2.041084	Non-race specific disease resistance protein 1; NDR1
Soltu.DM.08G013010	2.247632	1.939415	1.673427	Graves disease carrier protein; GDC
Soltu.DM.11G019760	5.340709	5.313257	4.738854	TMV resistance protein N
Soltu.DM.11G002030	1.714354	1.893802	1.687573	TMV resistance protein N
Soltu.DM.11G001930	1.670808	1.897231	1.711697	TMV resistance protein N
Soltu.DM.12G003210	1.809483	1.658407	1.67387	TMV resistance protein N
Soltu.DM.09G029660	1.656592	1.713184	1.572405	TMV resistance protein N
Soltu.DM.09G029410	1.73163	1.73163	1.204582	TMV resistance protein N
Soltu.DM.01G011420	1.377183	1.282032	1.348671	TMV resistance protein N
Soltu.DM.12G003230	1.217233	1.258855	1.322936	TMV resistance protein N
Soltu.DM.01G009400	-0.58349	-0.58763	-0.62739	Hypersensitive-induced response protein 1; HIR1
Soltu.DM.03G013090	-0.76825	-0.80305	-0.86986	Downy mildew resistance 6; DMR6
Soltu.DM.09G007070	0.92729	0.94126	0.95678	Pathogenesis-related leaf protein 4; P4

DOWN

Fig. 8. Differentially expressed pathogenesis-related genes in the leaves of the *DND1* silenced lines DND1-5, DND1-8 and DND1-17 compared to the non-transformed control 'Désirée' leaves. The intensity of colours indicates the degree of the difference (log2 fold change).

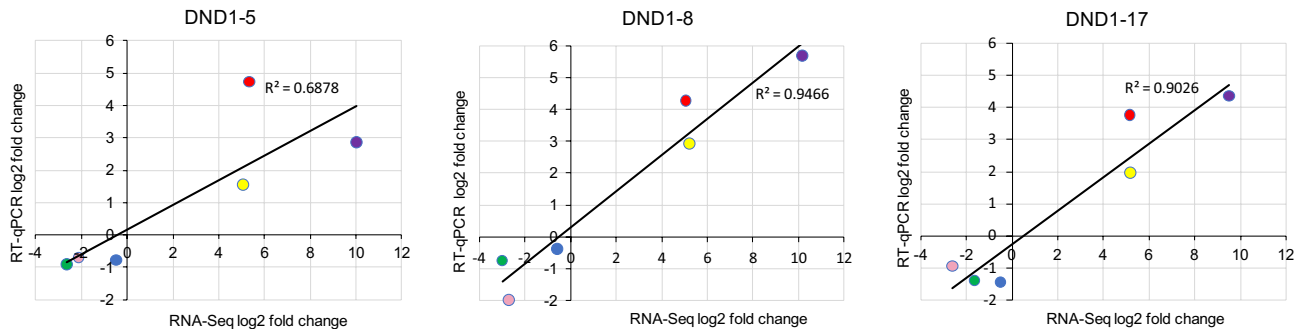


Fig. 9. Validation of RNA-seq results by correlation with RT-qPCR of six genes. The average log2 fold change in expression levels detected by RNA-seq of the two biological replicates is compared to the average log2 fold change in expression detected by RT-qPCR of three technical replicates of samples originating from independently grown in vitro plants. The selected genes were as follows: *PRO* (Soltu.DM.08G025180; green), *NR3* (Soltu.DM.11G013080; pink), *bHLH8* (Soltu.DM.01G047820; blue), *NAC90* (Soltu.DM.11G022040; yellow), *MLO6* (Soltu.DM.03G013460; red), *WRKY40* (Soltu.DM.08G015910; purple).

lines than in DES; this indicates that these branches of the phenylpropanoid pathway are repressed due to the silencing of *DND1*.

SA is synthesized via two pathways in plants: the isochorismate synthase (ICS) and phenylalanine ammonia-lyase (PAL) pathways²⁷. Isotope feeding experiments suggest that SA is synthesized by PAL from phenylalanine via *trans*-cinnamic acid and benzoic acid in the potato²⁸; however, the existence of the ICS pathway cannot be excluded. We found that not only the level of SA but also the amount of *para*-hydroxybenzoic acid (PBHA) was significantly increased in DND1 leaves. Because benzoic acid is a precursor of SA in the PAL pathway, the increased PBHA level detected in DND1 lines may support the previous finding that the bulk of SA is synthesized via PAL in the potato. Based on cDNA heterogeneity, it was estimated that at least about ten, but probably more, *PAL* genes are active in the potato²⁹. We found eleven, nine, and eight *PAL* genes in DND1-5, DND1-8, and DND1-17, respectively, with higher expression levels than in DES, out of which eight *PAL* alleles were common (Supplementary Table 9); this indicates a negative correlation between *DND1* function and *PAL* expression.

Based on *Arabidopsis* studies SA level is regulated by both positive and negative feedback. Briefly, *ICS1* expression in *Arabidopsis* is controlled mainly by SYSTEMIC ACQUIRED RESISTANCE DEFICIENT 1 (SARD1) and CALMODULIN BINDING PROTEIN 60 g (CBP60g) TFs. The TFs WRKY8, 28, 46, 48, and 75 and TEOSINTE BRANCHED1/CYCLOIDEA/PCF (TCP)-binding site TFs TCP8 and TCP9 promote *ICS1* expression, while ANAC019, 055, and 072, BENZOIC ACID/SA CARBOXYL METHYLTRANSFERASE 1 (BSMT1), ETHYLENE

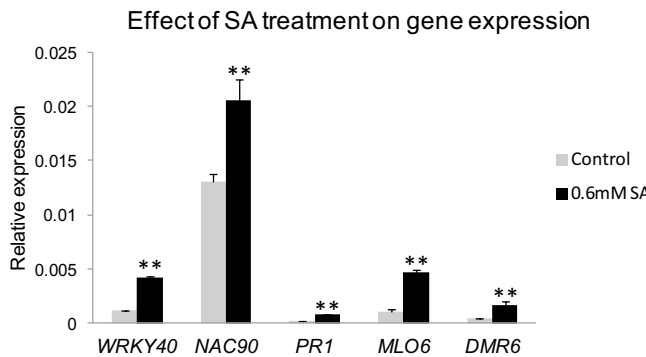


Fig. 10. Effect of exogenous salicylic acid (SA) treatment on the expression of five genes in the leaves of greenhouse-grown ‘Désirée’ plants. The relative expression level of the genes compared to the expression level of *ACTIN* was determined by RT-qPCR in three technical replicates. Three plants were treated with 0.6 mM SA as described in the Materials and methods. The standard deviations are indicated by the error bars. The statistical significance of the measurements was determined by Student’s *t*-test and labelled by ** ($p < 0.01$). *WRKY40* (Soltu.DM.08G015910) and *NAC90* (Soltu.DM.11G022040) are transcription factors whereas *PR1* (PATHOGENESIS-RELATED PROTEIN 1; Soltu.DM.01G045900), *MLO6* (MLO-LIKE PROTEIN 6; Soltu.DM.03G013460) and *DMR6* (DOWNY MILDEW RESISTANCE 6; Soltu.DM.06G028410) are related to pathogenesis.

INSENSITIVE 3 (EIN3) and EIN3-LIKE 1 (EIL1), and WRKY18, 40, 54, and 70 repress it³⁰. Out of these TFs, *WRKY48*, *WRKY75*, and *TCP8* were upregulated in *DND1* silenced potato lines with average fold changes of 39, 5.7, and 2.1 (Fig. 7), respectively, whereas only *EIL1* of the negative regulators appeared among the downregulated genes. Moreover, the level of *ICS* was not changed in *DND1* leaves compared to DES leaves, as it was not present among the DEGs, indicating that the ICS pathway of SA synthesis is much less significant in the potato than in *Arabidopsis*. Expression of *WRKY48* and *WRKY75* was connected to the JA signalling in *Catharanthus roseus* and the tomato, respectively^{31,32}, and this may also be the case in the potato.

In sum, 1866 common DEGs were detected in the *DND1* lines, and more than 60% (1138) of them were upregulated. The dominance of upregulation was particularly striking in the case of significant GO terms when it reached 91% (52/57). KEGG analysis pointed out that 80% (41/51) of the DEGs related to the biosynthesis of secondary metabolites were activated. Phenylpropanoids are derived from phenylalanine, and the first enzyme in the metabolism is *PAL*³³. Eight alleles of *PAL* are induced at 1.9- to 6.6-fold (Supplementary Table 9) in *DND1* lines, leading indirectly to the increase in the amount of chlorogenic acid and its derivatives (Fig. 2). Although we did not test the concentrations of flavonoids, several genes involved in flavonoid biosynthesis, e.g., *LEUCANTHOCYANIDIN DIOXYGENASE* (72-fold), *CAFFEOYL-CoA O-METHYLTRANSFERASE* (22-fold), and *FLAVONOID 3',5'-HYDROXYLASE* (4-fold), showed an elevated level of expression; this suggests an increase in concentration of a high range of flavonoids.

The most prominent enzymatic elements of the reactive oxygen species (ROS)-activated antioxidant plant defense machinery are PEROXIDASE, CATALASE, and SUPEROXIDE DISMUTASE³⁴. Interestingly, while the mRNA levels of PEROXIDASES increased by 5- to 26-fold, there was only a 1.4- to 1.8-fold increase in the expression of SUPEROXIDE DISMUTASE; a 1.4- to 1.5-fold reduction was detected in the transcript level of a CATALASE. Thus, we concluded that the silencing of *DND1* might not activate the antioxidant defense mechanism and the elevated level of PEROXIDASES might rather contribute to the increased phenypropanoid synthesis than to ROS elimination.

As in the case of the secondary metabolite metabolism, 80% (45/56) of the DEGs related to environmental adaptation were activated in the *DND1* lines. These include numerous alleles of *Mlo-like*, *LRK10L*, *Lr10*, *DMR6*, and *R1B* genes involved in plant-fungi interactions. However, members of the *MILDew LOCUS O* (*MLO*) gene family act as susceptibility factors by recognizing pathogens, and the corresponding loss-of-function mutations confer broad-spectrum durable host resistance³⁵. Furthermore, the mutated form of *DMR6* of *Arabidopsis* shows resistance to downy mildew³⁶. Thus, it is unlikely that the elevated expression of *Mlo-like* or *DMR6* would confer the reported late blight, powdery mildew, and gray mold resistance in the *DND1* lines. It is much more likely that the upregulation of *Lr10s*, *LRK10Ls*, and *R1Bs*, which are all resistance genes with proven effects against leaf rust in cereals and late blight in potato^{37–39}, contribute to the fungal resistance of the *DND1* silenced lines.

Infection of potato leaves with the late blight pathogen *P. infestans* leads to the massive accumulation of PR proteins⁴⁰, and several alleles of *PR* genes showed extreme expression in *DND1* lines. *PR-1* expression was up to more than 800-fold ($\log_2 = 9.8$ fold) higher in *DND1* lines than in the DES control (Fig. 8). Transgenic tobacco plants expressing the *PR-1a* gene at high levels have long been known to exhibit increased tolerance to *P. parasitica* and *Peronospora tabacina*⁴¹. Besides *PR-1*, *PR-2*, *4*, and *6* are activated in the *DND1* lines. *PR-2* is a β -1,3-glucanase and, in conjunction with *PR-1*, provides resistance against biotrophic fungi. *PR-4* is an endochitinase that aids in the degeneration of cell walls, while *PR-6* is a proteinase inhibitor⁴². It is known that *PR-1*, *2*, and *6* are regulated by SA⁴³. Thus, we assume that the increased level of SA activated the expression of *PR* genes in the *DND1* silenced lines.

The other well-known class of plant resistance proteins is the nucleotide-binding site and leucine-rich repeat domain proteins (NBS-LRRs), which are immune sensors and recognize the pathogen-derived molecules termed avirulence proteins⁴⁴. In rice, RGA4 and RGA5 act in interaction to mediate resistance to the fungal pathogen *Magnaporthe oryzae*. RGA4 is a trigger of cell death that is repressed in the presence of RGA5. Upon recognition of the pathogen effector by binding to RGA5, repression is relieved, and cell death occurs⁴⁵. In the DND1 lines, four alleles of *RGA4* showed a two to eightfold increase in expression, while *RGA5* was not among the DEGs. Thus, we assume that the uncontrolled activity of RGA4 could be one of the factors causing the leaf necrosis described in *DND1* silenced potato lines¹¹. Another factor might be the overexpression of the *HYPERSensitivity-INDUCED RESPONSE PROTEIN 1 (HIR1)* in DND1 lines, as this defense gene family is associated with hypersensitive reactions involving cell death and pathogen resistance^{46,47}. Notably, eight alleles of *TMV RESISTANCE PROTEIN N* were upregulated approximately 2- to 30-fold. This gene encodes a typical NBS-LRR protein that localizes TMV infection to cells adjacent to the site of viral entry and develops a hypersensitive response in the form of local necrotic lesions⁴⁸. Thus, the constitutive expression of *TMV RESISTANCE PROTEIN N* might be the third reason for leaf necrosis in DND1 lines.

DND1 is a cyclic nucleotide-gated ion channel protein². How can the reduced level of this protein cause changes in the expression level of almost 2000 genes? To answer this question, we tested the SA inducibility of five genes (*WRKY40, NAC90, PR1, MLO6, DMR6*) as representatives and predicted protein–protein interactions. All five genes, including the two TFs, turned out to be SA-activated. In total, twelve *WRKY* and eight *NAC* TF family members were induced in the DND1 lines. The role of *WRKY* TFs in regulating plant disease defense signalling is already well demonstrated in several plant species⁴⁹. In the potato, 110 *NAC* TF genes were identified, and seven of them were proven to improve the potato plant's ability to resist *Phytophthora* infection^{50,51}. Nevertheless, none of these seven genes were identical to those *NAC* genes that we identified as upregulated genes in the DND1 lines. The *bHLH* family members dominated the group of downregulated TFs. These TFs have a pleiotropic regulatory role in plant growth and development but are also involved in stress responses⁵². Thus, we assume that the downregulation of *bHLHs* would be one of the reasons for the retarded growth rate of *DND1* silenced lines. The predicted protein–protein interactions, however, did not show *WRKY*, *NAC*, or *bHLH* TFs as central proteins in the largest connected cluster, but some *WRKYs* had interactions with other *WRKYs*, such as, for example, *WRKY70* with *WRKY50* and *WRKY51* (Supplementary Table 8). The detected central proteins included histones, ubiquitin family proteins, kinases, heat shock, and brassinosteroid pathway-related proteins with very diverse and general functions. Thus, further studies would be necessary to elucidate the mechanism of how *DND1* influences the expression of approximately 2000 genes and the growth of plants.

Conclusion

Transcriptome, hormonal, and secondary metabolite analysis of the leaves of three in vitro-grown *DND1* silenced lines revealed a 10- to 20-fold increase in SA concentration that might be the major cause of transcriptional changes in almost 2000 genes. The upregulated expression of eight *PHENYLALANINE AMMONIA-LYASE (PAL)* genes and the unaltered level of *ISOCHORISMATE SYNTHASE (ICS)* mRNA supported the previous finding that, unlike in *Arabidopsis*, the bulk of SA is synthesized via *PAL* in potato. In correlation with *PAL* expression, the concentration of chlorogenic acid and its derivatives was increased, but the antioxidant defense mechanism was not activated. Several resistance genes, including *Lr10s*, *LRK10Ls*, *R1Bs*, and *PRs*, were upregulated, which might be the main factor behind fungal resistance, while the overexpression of the *R-GENE ANALOG 4 (RGA4)*, *HYPERSensitivity-INDUCED RESPONSE PROTEIN 1 (HIR1)*, and *TMV RESISTANCE PROTEIN N* might explain the existence of local necrotic lesions in the leaves of *DND1* silenced lines. Dominated by *WRKYs* and *NACs*, 60 upregulated TF genes were identified, whereas in the group of 63 downregulated TF genes, the *bHLHs* were in excess. Because *bHLHs* highly influence plant growth and development, we hypothesize that their downregulation is a key factor in turning the *DND1* plants from growth to defense.

Materials and methods

Plant materials and growth conditions

The *DND1* silenced lines DND1-5, DND1-8, and DND1-17 were previously generated from *Solanum tuberosum* cv. 'Désirée'¹¹ and transferred to our laboratory via authorized transboundary movement. They were propagated in vitro in rooting medium RM (MS⁵³ without vitamins containing 2% (w/v) sucrose and 0.8% (w/v) agar) at 24 °C with a 16-h photoperiod at a light intensity of 75 $\mu\text{mol m}^{-2} \text{s}^{-1}$ for 4 weeks in 40-mL test tubes closed with paper plugs and transferred into pots containing Tabaksubstrat sterile soil A200 (Stender GmbH, Schermbeck, Germany). The plants in pots were grown under greenhouse conditions at a temperature regime of 18–24 °C and a 16 h/8 h day/night photoperiod. Soil humidity was approximately 80%. Plants were irrigated according to need and treated weekly with acetamiprid-containing pesticide (Mospilan 20 SG).

Salicylic acid treatment

To study the effect of the exogenous salicylic acid (SA) on gene expression, 4-week-old pot-grown 'Désirée' plants were treated with 30 mL of 0.6 mM SA⁵⁴ (S1367, Duchefa Biochemie, Haarlem, The Netherlands) solution using a hand sprayer with a full cone nozzle. For the control treatment, deionized water spraying was applied. Foliar spraying was done at 11:00 am and 3:00 pm. Three plants were subjected to both the SA and control treatments. Twenty-four hours after the first foliar spraying, three leaves from each plant were collected for target gene expression analysis. Leaf samples were frozen in liquid nitrogen and stored at –80 °C until processing.

Targeted metabolite analysis

Ultra-performance liquid chromatography–tandem mass spectrometry (UPLC–MS/MS) was used to detect general phenolics and plant hormones in the leaves of 4-week-old in vitro plants as described earlier⁵⁵. Briefly, frozen leaves were ground in a mortar with a pestle. Samples were spiked with labelled [³H₆](-)-*cis*, *trans*-abscisic acid as an internal standard and extracted with methanol:water (2:1) with vigorous shaking. Then, samples were filtered through a 0.22-μm PTFE syringe filter and submitted for analysis. Separation was achieved on an Acuity I class UPLC system (Waters, Milford, MA, USA) on a Waters HSS T3 column (1.8 μm, 100 mm × 2.1 mm). Gradient elution was used with 0.1% (v/v) formic acid in both water (A) and acetonitrile (B). Tandem mass spectrometric detection was performed on a Waters Xevo TQ-XS equipped with a UniSpray™ source operated in timed multiple reaction monitoring mode.

Transcriptome analysis

RNA was isolated⁵⁶ from a pool of 15 leaves harvested from five 4-week-old in vitro plants. Two independent pools were prepared from each *DND1* silenced line and the control ‘Désirée’ RNA samples were transported to the Novogene Company Ltd. (Cambridge, UK) and used for quality control and the generation of sequencing libraries. A 150-bp paired-end sequencing strategy (Illumina NovaSeq 6000 platform) was carried out followed by a quality check of the resulting data. The basic bioinformatic analysis including mapping of quality reads (FPKM, Fragments Per Kilobase Million) to the latest version (v.6.1) of the *S. tuberosum* group Phureja DM1-3 reference genome⁵⁷ (http://solanaceae.plantbiology.msu.edu/dm_v6_1_download.shtml), gene expression level analysis (e.g., coexpression Venn diagram; Fig. 3a), and differential gene expression analysis (log₂ fold change of DEGs, Supplementary Tables 3–5 and volcano plot, Supplementary Fig. 2) were also performed by the company Novogene.

The functional annotation of the network nodes (DEGs) followed a 3-way approach. First, to determine functional domains from DEGs, their associated amino acid sequences were scanned with the Hidden Markov Model (HMM)-based HMMER v3.3.2 software package⁵⁸ using Pfam-A v35.0 HMM profiles (<ftp://ftp.ebi.ac.uk>). Second, for gene ontology (GO) analysis, an up-to-date ontology database (<http://geneontology.org/docs/download-ontology>; go-basic) and custom-made gene annotation dataset were assembled based on ontology information of the Universal Protein Resource (ftp://ftp.uniprot.org/pub/databases/uniprot/previous_releases/release-2019_04/). The enrichment analysis was performed with the BiNGO v3.0.3 plug-in⁵⁹ to the Cytoscape v3.7.2 software⁶⁰. Over-represented GO terms were determined using a hypergeometric statistical test with Benjamini and Hochberg False Discovery Rate (FDR) correction at a *p* ≤ 0.0001 significance level. Then, REVIGO⁶¹ was used with default settings (simrel; 0.7) to reduce the GO term list. Datasets from the GO enrichment analysis were visualized with the ggplot2 R-package (<https://github.com/tidyverse/ggplot2>). Finally, the Wget software package (<https://www.gnu.org/software/wget>) was used to retrieve the corresponding datasets from the KEGG knowledgebase⁶², including functional annotations, metabolic pathway classifications, and nucleotide/protein sequences.

Potato-related protein–protein interaction data were retrieved from the STRING database⁶³. Specific identifiers among the various potato genome projects (SpudDB, <http://spuddb.uga.edu/index.shtml> and the PGSC Ensembl database https://plants.ensembl.org/Solanum_tuberosum/Info/Index) were clarified based on the homology of sequences using the BLASTP tool⁶⁴. Network topology was designed and visualized with yEd Graph Editor software version 3.23.1 (<https://www.yworks.com/products/yed>). The source code (graphml) of the graphs was deposited to GitHub Gist and is accessible online via yEd Live (<https://bit.ly/3tLMqbH>).

Targeted gene expression analysis

The total RNA purified from 150 mg of frozen leaf tissues⁵⁶ was dissolved in 30 μL of deionized water, and the concentration was measured at OD₂₆₀ using an ND-1000 Nanodrop spectrophotometer (Thermo Fisher Scientific, Waltham, MA, USA).

The expression level of *DND1* in the silenced lines DND1-5, DND1-8, and DND1-17 compared to the non-transformed control ‘Désirée’ was tested in cDNA samples reverse transcribed from the RNA samples (1000 ng) with a RevertAid First Strand cDNA Synthesis Kit (Thermo Fisher Scientific) using random primers. The cDNA samples were diluted threefold, and 0.6 μL was added as a template into 10-μL qPCR reactions. Primers were used in 1 μM final concentration each at a melting temperature of 60 °C together with the Fast SYBR® GreenMaster Mix (Applied Biosystems, Waltham, MA, USA). qPCRs were carried out in triplicates in a Fast 7500 instrument (Applied Biosystems). The housekeeping potato gene *ELONGATION FACTOR 1α* was used as the reference gene. The transcription level was calculated using the 2^{-ΔΔC_T} method⁶⁵ with efficiency correction according to Pfaffl⁶⁶.

For validation of RNA-seq results RNA was isolated from the leaves of a new generation of in vitro plants. RT–qPCR analysis was conducted with 2 μL of total RNA using the GoTaq® 1-Step RT–qPCR System kit (Promega Corporation, Madison, WI, USA). Standard cycling conditions of 3-step amplification were started at 37 °C for 15 min and 95 °C for 10 min, then followed by 40 cycles of 95 °C for 10 s, 60 °C for 30 s, and 72 °C for 30 s. To test the effect of SA treatment, the cDNA was synthesized using the Maxima H minus First Strand cDNA Synthesis Kit with dsDNase according to the manufacturer’s (Thermo Fisher Scientific) instructions. RT–qPCR assays were performed with 2 μL of cDNA using the Xpert Fast SYBR (uni) 2× Master mix (GRiSP Research Solutions, Porto, Portugal) under the following thermal conditions: 95 °C for 3 min followed by 40 cycles of 95 °C for 5 s, 60 °C for 30 s, and 72 °C for 30 s. Both RT–qPCR experiments were carried out in a Light Cycler-96 Thermal cycler and analyzed using the Light Cycler-96 Software version 1.1 (Roche Diagnostics GmbH, Mannheim, Germany). *ACTIN* was used as a reference gene⁶⁷ in both experiments.

Primers (Supplementary Table 10) were designed using the NIH Primer-BLAST tool (<https://www.ncbi.nlm.nih.gov/tools/primer-blast/>) with default parameters.

Statistical analysis

Calculation of log2 fold changes and correlation parameters was done by using the MS Excel 2023 software. The statistical significance of the measurements was determined by Student's *t*-test at the $p < 0.01$ and $p < 0.05$ levels.

Data availability

RNA-seq raw data were deposited at ArrayExpress (E-MTAB-13824) and European Nucleotide Archive (ERP157543), and can be reached at <https://www.ebi.ac.uk/biostudies/arrayexpress/studies/E-MTAB-13824?key=9a3f8423-d58e-4563-9cf8-71b1e7807014>. All other data generated or analysed during this study are included in this published article and its supplementary information files.

Received: 3 May 2024; Accepted: 27 August 2024

Published online: 04 September 2024

References

- Pavan, S., Jacobsen, E., Visser, R. G. F. & Bai, Y. Loss of susceptibility as a novel breeding strategy for durable and broad-spectrum resistance. *Mol. Breed.* **25**, 1–12 (2010).
- Clough, S. J. *et al.* The *Arabidopsis dnd1* defense, no death gene encodes a mutated cyclic nucleotide-gated ion channel. *Proc. Natl. Acad. Sci. U.S.A.* **97**, 9323–9328 (2000).
- Yu, I.-C., Parker, J. & Bent, A. F. Gene-for-gene disease resistance without the hypersensitive response in *Arabidopsis dnd1* mutant. *Proc. Natl. Acad. Sci. U.S.A.* **95**, 7819–7824 (1998).
- Genger, R. K. *et al.* Signaling pathways that regulate the enhanced disease resistance of *Arabidopsis* defense, no death mutants. *Mol. Plant Microbe Interact.* **21**, 1285–1296 (2008).
- Ali, R. *et al.* Death don't have no mercy and neither does calcium: *Arabidopsis* CYCLIC NUCLEOTIDE GATED CHANNEL2 and innate immunity. *Plant Cell* **19**, 1081–1095 (2007).
- Ma, W. *et al.* Leaf senescence signaling: The Ca^{2+} -conducting *Arabidopsis* cyclic nucleotide gated channel2 acts through nitric oxide to repress senescence programming. *Plant Physiol.* **154**, 733–743 (2010).
- Ma, W. & Berkowitz, G. A. Cyclic nucleotide gated channel and Ca^{2+} -mediated signal transduction during plant senescence signaling. *Plant Signal Behav.* **6**, 413–415 (2011).
- Chin, K., DeFalco, T. A., Moeder, W. & Yoshioka, K. The *Arabidopsis* cyclic nucleotide-gated ion channels AtCNGC2 and AtCNGC4 work in the same signaling pathway to regulate pathogen defense and floral transition. *Plant Physiol.* **163**, 611–624 (2013).
- Fortuna, A. *et al.* Crossroads of stress responses, development and flowering regulation—The multiple roles of Cyclic Nucleotide Gated Ion Channel 2. *Plant Signal. Behav.* **10**, e989758 (2015).
- Fernandez, D. *et al.* Coffee (*Coffea arabica* L.) genes early expressed during infection by the rust fungus (*Hemileia vastatrix*). *Mol. Plant Pathol.* **5**, 527–536 (2004).
- Sun, K. *et al.* Down-regulation of *Arabidopsis DND1* orthologs in potato and tomato leads to broad-spectrum resistance to late blight and powdery mildew. *Transgenic Res.* **25**, 123–138 (2016).
- Sun, K. *et al.* Silencing of *DND1* in potato and tomato impedes conidial germination, attachment and hyphal growth of *Botrytis cinerea*. *BMC Plant Biol.* **17**, 235 (2017).
- Kieu, N. P., Lenman, M., Wang, E. S., Petersen, B. L. & Andreasson, E. Mutations introduced in susceptibility genes through CRISPR/Cas9 genome editing confer increased late blight resistance in potatoes. *Sci. Rep.* **11**, 4487 (2021).
- Kapoor, B., Kumar, P., Sharma, R. & Kumar, A. Regulatory interactions in phytohormone stress signaling implying plants resistance and resilience mechanisms. *J. Plant Biochem. Biotechnol.* **30**, 813–828 (2021).
- Zaynab, M. *et al.* Role of secondary metabolites in plant defense against pathogens. *Microb. Pathog.* **124**, 198–202 (2018).
- Kanehisa, M. & Goto, S. KEGG: Kyoto encyclopedia of genes and genomes. *Nucleic Acids Res.* **28**, 27–30 (2000).
- Gupta, R., Anand, G. & Bar, M. Developmental phytohormones: Key players in host–microbe interactions. *J. Plant Growth Reg.* **42**, 7330–7351 (2023).
- Dong, J., Chen, C. & Chen, Z. Expression profiles of the *Arabidopsis* WRKY gene superfamily during plant defense response. *Plant Mol. Biol.* **51**, 21–37 (2003).
- Uknes, S. *et al.* Acquired resistance in *Arabidopsis*. *Plant Cell* **4**, 645–656 (1992).
- Gruner, K., Zeier, T., Aretz, C. & Zeier, J. A critical role for *Arabidopsis MILDEW RESISTANCE LOCUS O2* in systemic acquired resistance. *Plant J.* **94**, 1064–1082 (2018).
- Zeilmaker, *et al.* Downy mildew resistant 6 and DMR6-like oxygenase 1 are partially redundant but distinct suppressors of immunity in *Arabidopsis*. *Plant J.* **81**, 210–222 (2015).
- Song, W., Shao, H., Zheng, A., Zhao, L. & Xu, Y. Advances in roles of salicylic acid in plant tolerance responses to biotic and abiotic stresses. *Plants* **12**, 3475 (2023).
- Macioszek, V. K., Jęcz, T., Ciereszko, I. & Kononowicz, A. K. Jasmonic acid as a mediator in plant response to necrotrophic fungi. *Cells* **12**, 1027 (2023).
- Fu, W. *et al.* The jasmonic acid-amino acid conjugates JA-Val and JA-Leu are involved in rice resistance to herbivores. *Plant Cell Environ.* **45**, 262–272 (2022).
- Jeyasri, R. *et al.* Methyl jasmonate and salicylic acid as powerful elicitors for enhancing the production of secondary metabolites in medicinal plants: An updated review. *Plant Cell Tissue Organ Cult.* **153**, 447–458 (2023).
- Kabir, F., Katayama, S., Tanji, N. & Nakamura, S. Antimicrobial effects of chlorogenic acid and related compounds. *J. Korean Soc. Appl. Biol. Chem.* **57**, 359–365 (2014).
- Chen, Z., Zheng, Z., Huang, J., Lai, Z. & Fan, B. Biosynthesis of salicylic acid in plants. *Plant Signal Behav.* **4**, 493–496 (2009).
- Coquoz, J. L., Buchala, A. & Metraux, J. P. The biosynthesis of salicylic acid in potato plants. *Plant Physiol.* **117**, 1095–1101 (1998).
- Joos, H.-J. & Hahlbrock, K. Phenylalanine ammonia-lyase in potato (*Solanum tuberosum* L.): Genomic complexity, structural comparison of two selected genes and modes of expression. *Eur. J. Biochem.* **204**, 621–629 (1992).
- Huang, W., Wang, Y., Li, X. & Zhang, Y. Biosynthesis and regulation of salicylic acid and N-hydroxyproline in plant immunity. *Mol. Plant* **13**, 31–41 (2020).
- Schluttenhofer, C., Pattanaik, S., Patra, B. & Yuan, L. Analyses of *Catharanthus roseus* and *Arabidopsis thaliana* WRKY transcription factors reveal involvement in jasmonate signaling. *BMC Genom.* **15**, 502 (2014).
- López-Galiano, M. J. Epigenetic regulation of the expression of WRKY75 transcription factor in response to biotic and abiotic stresses in Solanaceae plants. *Plant Cell Rep.* **37**, 167–176 (2018).
- Obata, T. Metabolons in plant primary and secondary metabolism. *Phytochem. Rev.* **18**, 1483–1507 (2019).
- Kesawat, M. S. *et al.* Regulation of reactive oxygen species during salt stress in plants and their crosstalk with other signaling molecules—Current perspectives and future directions. *Plants* **12**, 864 (2023).
- Kusch, S. & Panstruga, R. Mlo-based resistance: An apparently universal weapon to defeat powdery mildew disease. *Mol. Plant Microbe Interact.* **30**, 179–189 (2017).

36. Van Damme, M. *et al.* Identification of *Arabidopsis* loci required for susceptibility to the downy mildew pathogen *Hyaloperonospora parasitica*. *Mol. Plant Microbe Interact.* **18**, 583–592 (2005).
37. Schachermayr, G., Feuillet, C. & Keller, B. Molecular markers for the detection of the wheat leaf rust resistance gene *Lr10* in diverse genetic backgrounds. *Mol. Breed.* **3**, 65–74 (1997).
38. Feuillet, C., Schachermayr, G. & Keller, B. Molecular cloning of a new receptor-like kinase gene encoded at the *Lr10* disease resistance locus of wheat. *Plant J.* **11**, 45–52 (1997).
39. Tiwari, J. K. *et al.* Genome sequence analysis provides insights on genomic variation and late blight resistance genes in potato somatic hybrid (parents and progeny). *Mol. Biol. Rep.* **48**, 623–635 (2021).
40. Hoegen, E., Strömberg, A., Pihlgren, U. & Kombrink, E. Primary structure and tissue-specific expression of the pathogenesis-related protein PR-1b in potato. *Mol. Plant Pathol.* **3**, 329–345 (2002).
41. Alexander, D. *et al.* Increased tolerance to two oomycete pathogens in transgenic tobacco expressing pathogenesis-related protein 1a. *Proc. Natl. Acad. Sci. U.S.A.* **90**, 7327–7331 (1993).
42. Islam, M. M. *et al.* Pathogenesis-related proteins (PRs) countering environmental stress in plants: A review. *S. Afr. J. Bot.* **160**, 414–427 (2023).
43. Sudisha, J., Sharathchandra, R. G., Amruthesh, K. N., Kumar, A. & Shetty, H. S. Pathogenesis related proteins in plant defence response. In *Plant Defence: Biological Control* (eds Mérillon, J. M. & Ramawat, K. G.) 379–403 (Springer, 2011).
44. Tailor, A. & Bhatla, S. C. R gene-mediated resistance in the management of plant diseases. *J. Plant Biochem. Biotechnol.* **33**, 5–23 (2024).
45. Césari, S. *et al.* The NB-LRR proteins RGA4 and RGA5 interact functionally and physically to confer disease resistance. *EMBO J.* **33**, 1941–1959 (2014).
46. Nadimpalli, R., Yalpani, N., Johal, G. S. & Simmons, C. R. Prohibitins, stomatin, and plant disease response genes compose a protein superfamily that controls cell proliferation, ion channel regulation, and death. *J. Biol. Chem.* **275**, 29579–29586 (2000).
47. Jung, H. W. & Hwang, B. K. The leucine-rich repeat (LRR) protein, CaLRR1, interacts with the hypersensitive induced reaction (HIR) protein, CaHIR1, and suppresses cell death induced by the CaHIR1 protein. *Mol. Plant Pathol.* **8**, 503–514 (2007).
48. Erickson, F. L. *et al.* The helicase domain of the TMV replicase proteins induces the N-mediated defense response in tobacco. *Plant J.* **18**, 67–75 (1999).
49. Saha, B. *et al.* Unraveling the involvement of WRKY TFs in regulating plant disease defense signaling. *Planta* **259**, 7 (2024).
50. Singh, A. K., Sharma, V., Pal, A. K., Acharya, V. & Ahuja, P. S. Genome-wide organization and expression profiling of the NAC transcription factor family in potato (*Solanum tuberosum* L.). *DNA Res.* **20**, 403–423 (2013).
51. Collinge, M. & Boller, T. Differential induction of two potato genes, *Stpx2* and *StNAC*, in response to infection by *Phytophthora infestans* and to wounding. *Plant Mol. Biol.* **46**, 521–529 (2001).
52. Hao, Y., Zong, X., Ren, P., Qian, Y. & Fu, A. Basic helix-loop-helix (bHLH) transcription factors regulate a wide range of functions in *Arabidopsis*. *Int. J. Mol. Sci.* **22**, 7152 (2021).
53. Murashige, T. & Skoog, F. A revised medium for rapid growth and bioassays with tobacco tissue cultures. *Physiol. Plant.* **15**, 473–497 (1962).
54. Li, Q. *et al.* Foliar application of salicylic acid alleviate the cadmium toxicity by modulation the reactive oxygen species in potato. *Ecotoxicol. Environ. Saf.* **172**, 317–325 (2019).
55. Jose, J. *et al.* Global transcriptome and targeted metabolite analyses of roots reveal different defence mechanisms against *Ralstonia solanacearum* infection in two resistant potato cultivars. *Front. Plant Sci.* **13**, 1065419 (2023).
56. Stiekema, W. J. *et al.* Molecular cloning and analysis of four potato tuber mRNAs. *Plant Mol. Biol.* **11**, 255–269 (1988).
57. Pham, G. M. *et al.* Construction of a chromosome-scale long-read reference genome assembly for potato. *GigaScience* **9**, giaa100 (2020).
58. Eddy, S. R. A new generation of homology search tools based on probabilistic inference. *Genome Inform.* **23**, 205–211 (2009).
59. Maere, S., Heymans, K. & Kuiper, M. BiNGO: A Cytoscape plugin to assess overrepresentation of gene ontology categories in biological networks. *Bioinformatics* **21**, 3448–3449 (2005).
60. Shannon, P. *et al.* Cytoscape: A software environment for integrated models of biomolecular interaction networks. *Genome Res.* **13**, 2498–2504 (2003).
61. Supek, F., Bošnjak, M., Škunca, N. & Šmuc, T. REVIGO summarizes and visualizes long lists of gene ontology terms. *PLoS ONE* **6**, e21800 (2011).
62. Kanehisa, M., Goto, S., Sato, Y., Furumichi, M. & Tanabe, M. KEGG for integration and interpretation of large-scale molecular data sets. *Nucleic Acids Res.* **40**, D109–D114 (2012).
63. Szklarczyk, D. *et al.* The STRING database in 2023: Protein–protein association networks and functional enrichment analyses for any sequenced genome of interest. *Nucleic Acids Res.* **51**, D638–D646 (2023).
64. Camacho, C. *et al.* BLAST+: Architecture and applications. *BMC Bioinform.* **10**, 421 (2009).
65. Livak, K. J. & Schmittgen, T. D. Analysis of relative gene expression data using real-time quantitative PCR and the $2^{-\Delta\Delta C_T}$ method. *Methods* **25**, 402–408 (2001).
66. Pfaffl, M. W. Quantification strategies in real-time PCR. In *A-Z of Quantitative PCR* (ed. Bustin, S. A.) 89–113 (FIVephoton Biochemicals, 2004).
67. Nicot, N., Hausman, J. F., Hoffmann, L. & Evers, D. Housekeeping gene selection for real-time RT-PCR normalization in potato during biotic and abiotic stress. *J. Exp. Bot.* **56**, 2907–2914 (2005).

Acknowledgements

The authors sincerely thank Prof. R. G. F. Visser (WUR, Wageningen, The Netherlands) for generously providing the DND1 silenced potato lines. We thank Monika Kiss for the excellent technical assistance and plant propagation. Funding support for this work was provided by the National Research, Development and Innovation Office, Budapest, Hungary (Grant Nos. K_132967 and RRF-2.3.1-21-2022-00007).

Author contributions

Z.B. conceived and designed the study, participated in the data analysis, and wrote the manuscript; B.K. performed the GO, KEGG and protein–protein interaction studies; K.Á.H. conducted the hormone and metabolite measurements; J.J., C.É. and K.O. performed the gene expression studies, F.K.-R. and V.V. participated in transcriptome data analysis and presentation; L.S. supervised the study with Z.B. and edited the manuscript. All authors have read and approved the final version of the manuscript.

Competing interests

The authors declare no competing interests.

Additional information

Supplementary Information The online version contains supplementary material available at <https://doi.org/10.1038/s41598-024-71380-9>.

Correspondence and requests for materials should be addressed to Z.B.

Reprints and permissions information is available at www.nature.com/reprints.

Publisher's note Springer Nature remains neutral with regard to jurisdictional claims in published maps and institutional affiliations.

Open Access This article is licensed under a Creative Commons Attribution-NonCommercial-NoDerivatives 4.0 International License, which permits any non-commercial use, sharing, distribution and reproduction in any medium or format, as long as you give appropriate credit to the original author(s) and the source, provide a link to the Creative Commons licence, and indicate if you modified the licensed material. You do not have permission under this licence to share adapted material derived from this article or parts of it. The images or other third party material in this article are included in the article's Creative Commons licence, unless indicated otherwise in a credit line to the material. If material is not included in the article's Creative Commons licence and your intended use is not permitted by statutory regulation or exceeds the permitted use, you will need to obtain permission directly from the copyright holder. To view a copy of this licence, visit <http://creativecommons.org/licenses/by-nc-nd/4.0/>.

© The Author(s) 2024